(7) M. H. Chisholm and H. C. Clark, *Inorg. Chem.*, **10**, 1711 (1971).
(8) M. H. Chisholm and H. C. Clark, *J. Chem. Soc., Chem. Commun.*, 1484 (1972).
(9) M. H. Chisholm, H. C. Clark, L. E. Manzer, and J. B. Stothers, *Chem. Commun.*, 1627 (1971).
(10) J. A. Connor, E. M. Jones, E. W. Randall, and E. Rosenberg, *J. Chem. Soc., Dalton Trans.*, 2419 (1972).
(11) C. G. Kreiter and V. Formáček, *Angew. Chem., Int. Ed. Engl.*, **11**, 141 (1972).
(12) H. Werner, E. O. Fischer, B. Heckel, and C. G. Kreiter, *J. Organometal. Chem.*, **28**, 367 (1971).
(13) J. A. Connor and E. O. Fischer, *J. Chem. Soc. A*, 578 (1969).
(14) E. Moser and E. O. Fischer, *J. Organometal. Chem.*, **13**, 387 (1968).
(15) T. G. Appleton, M. H. Chisholm, H. C. Clark, and K. Yasufuku, *J. Amer. Chem. Soc.*, in press.
(16) No simple organoplatinum(II) compounds PtR(COCH$_3$)L$_2$ are known. We would expect that complexes of this type would be labile due to the mutually high trans influences of the two trans Pt–C bonds and thus that they would readily decompose either by reaction with the solvent or by reductive elimination.
(17) F. A. Cotton and C. M. Lukehart, *J. Amer. Chem. Soc.*, **93**, 2672 (1971).
(18) F. A. Cotton and C. M. Lukehart, *J. Amer. Chem. Soc.*, **95**, 3552 (1973).
(19) J. Halpern, *Accounts Chem. Res.*, **3**, 386 (1970).
(20) T. G. Appleton, H. C. Clark, and L. E. Manzer, *Inorg. Chem.*, in press.
(21) M. H. Chisholm, H. C. Clark, and L. E. Manzer, *Inorg. Chem.*, **11**, 1269 (1972).
(22) T. G. Appleton, H. C. Clark, and L. E. Manzer, *Coord. Chem. Rev.*, **10**, 335 (1973).

---

Contribution from the Department of Chemistry,
Northern Illinois University, DeKalb, Illinois 60115

# Electronic Structure and Spectra of Square-Planar Cyano and Cyanoamine Complexes of Platinum(II)[1]

HUSEYIN ISCI and W. ROY MASON*

*Received June 18, 1974* AIC403915

Solution electronic absorption and magnetic circular dichroism (MCD) spectral measurements are reported for Pt(CN)$_4^{2-}$, *cis-* and *trans*-Pt(NH$_3$)$_2$(CN)$_2$, Pt(en)(CN)$_2$, and Pt(*l*-pn)(CN)$_2$, together with some absorption spectral data for the Pt(dien)(CN)$^+$ ion. In addition, some low-temperature (26°K) absorption data are given for Pt(CN)$_4^{2-}$, *trans*-Pt(NH$_3$)$_2$(CN)$_2$, and Pt(en)(CN)$_2$ in poly(vinyl alcohol) (PVA) solid films prepared from aqueous PVA solutions. The cyanoamine complexes exhibit intense absorptions between 35 and 54 kK, similar to those observed for Pt(CN)$_4^{2-}$. These transitions are ascribed to metal → ligand (M → L) charge transfer from occupied metal d orbitals to the lowest energy $\pi^*$ CN$^-$ orbital. In addition, the *trans*-Pt(NH$_3$)$_2$(CN)$_2$ and Pt(dien)(CN)$^+$ complexes show an allowed d → p transition above 50 kK. The M → L spectra are interpreted by means of a model which involves a single $\pi^*$ CN$^-$ acceptor orbital and which includes metal spin–orbit coupling in the M → L excited states. Some spin–orbit calculations are presented for Pt(CN)$_4^{2-}$, *trans*-Pt(NH$_3$)$_2$(CN)$_2$, and Pt(en)(CN)$_2$. Spectral assignments are given for each complex and the results are discussed in terms of d-orbital participation in bonding and in terms of the donor–acceptor character of the CN$^-$ ligand.

## Introduction

During the last 1.5 decades, there have been a number of investigations aimed at characterizing the electronic structure of the Pt(CN)$_4^{2-}$ ion and interpreting its electronic absorption and magnetic circular dichroism (MCD) spectra.[2-9] In spite of this effort, a model free of disagreement has failed to emerge, and the ordering of excited states accessible to optical transitions remains controversial. This is unfortunate because Pt(CN)$_4^{2-}$ is a prototypical planar cyano complex and might easily serve as a model for other planar complexes which contain $\pi$-acid ligands and which exhibit metal–ligand (M → L) bonding and charge-transfer spectra.

There have been two main points of disagreement in describing the electronic structure of the Pt(CN)$_4^{2-}$ ion: (1) the ordering of the occupied metal d molecular orbitals and their participation in bonding and (2) the extent to which the several empty, low-lying $\pi^*$ CN$^-$ molecular orbitals are involved in electronic transitions. For example, the three lowest energy absorption bands at 35.7, 39.1, and 41.3 kK in the solution electronic spectra were interpreted by Gray and Ballhausen[3] as M → L transitions from the occupied d orbitals to a single $\pi^*$ CN$^-$ orbital, $a_{2u}(\pi^*)$. Their ordering of excited states implied the ordering of the occupied d levels as $d_{xy} > d_{xz}d_{yz} > d_{z^2}$, assuming negligible electronic repulsion differences. Moncuit[4] interpreted the electronic spectra, including an intense band at 46.3 kK in terms of M → L transitions to three $\pi^*$ CN$^-$ orbitals, $a_{2u}(\pi^*)$, $e_u(\pi^*)$, and $b_{2u}(\pi^*)$, and proposed the ordering $d_{xy} > d_{z^2} > d_{xz}d_{yz}$. Mason and Gray[5] assigned the low-temperature (77°K) EPA solution spectra using two $\pi^*$ cyanide orbitals, $a_{2u}(\pi^*)$ and $e_u(\pi^*)$, and the original ordering of the d levels of Gray and Ballhausen. Piepho, Schatz, and McCaffery[6] analyzed the MCD spectra of the Pt(CN)$_4^{2-}$ ion and offered an interpretation involving M → L transitions to the $a_{2u}(\pi^*)$ level but included spin–orbit coupling in excited states. As a consequence of spin–orbit coupling, formally spin-forbidden transitions were assumed to gain considerable intensity. The implied ordering of the d levels was $d_{z^2} \sim d_{xz}d_{yz} > d_{xy}$. Still other spectral interpretations and d-level orderings have been proposed[8] from studies on solid salts of Pt(CN)$_4^{2-}$, but it seems clear that strong, specific solid-state perturbations are present in these cases because of features of the crystals which allow close platinum–platinum contact.[9,10]

In order to learn more about the bonding in planar cyano complexes and to provide an experimental basis for further discussion of the Pt(CN)$_4^{2-}$ problem, we have investigated a number of related cyanoamine complexes of platinum(II) and have compared them with Pt(CN)$_4^{2-}$. Solution electronic absorption and MCD spectra were obtained for *cis-* and *trans*-Pt(NH$_3$)$_2$(CN)$_2$, Pt(en)(CN)$_2$, and Pt(*l*-pn)(CN)$_2$; some absorption spectra were also obtained for the Pt(dien)(CN)$^+$ ion. In addition, some low-temperature (26°K) measurements were also made for Pt(CN)$_4^{2-}$, *trans*-Pt(NH$_3$)$_2$(CN)$_2$, and Pt(en)(CN)$_2$ in solid poly(vinyl alcohol) (PVA) films prepared from aqueous PVA solutions. These spectra were interpreted using the model developed by Piepho, *et al.*,[6] for Pt(CN)$_4^{2-}$, which includes spin–orbit coupling in excited states and involves only a single $\pi^*$ CN$^-$ level for excited configurations.

## Experimental Section

**Preparation of Compounds.** The starting material for the platinum complexes was H$_2$PtCl$_4$, a solution of which was prepared from platinum sponge.[11] Potassium tetracyanoplatinate(II), K$_2$[Pt(CN)$_4$], and the tetra-*n*-butylammonium salt were prepared according to the literature.[5,12] All other chemicals were of reagent grade unless otherwise noted.

***trans*-Dicyanodiammineplatinum(II), *trans*-$Pt(NH_3)_2(CN)_2$.**[13] A stoichiometric amount of $AgNO_3$ (2:1 molar ratio) was added to a suspension of *trans*-$Pt(NH_3)_2Cl_2$[14] in water and the resulting mixture was stirred at boiling temperature for 30 min. After cooling to ice-bath temperature, the silver chloride was removed by filtration, and the colorless filtrate was treated with a stoichiometric amount of potassium cyanide. Needlelike white crystals were formed when the solution was maintained at ice-bath temperature overnight. The crystals were collected by suction filtration, washed with ice-cold absolute ethanol and ether, and then dried in a vacuum desiccator overnight. *Anal.* Calcd for $Pt(NH_3)_2(CN)_2$: C, 8.54; H, 2.15; N, 19.93; Pt, 69.38. Found: C, 8.51; H, 2.11; N, 19.77; Pt, 69.54. Ir: $\bar{\nu}_{CN}$ 2130 $cm^{-1}$.

***cis*-Dicyanodiammineplatinum(II), *cis*-$Pt(NH_3)_2(CN)_2$.**[15] Platinum(II) cyanide[16] was dissolved in concentrated aqueous ammonia solution by boiling and stirring for about 1 hr. The solution was filtered while hot, and a white crystalline solid precipitated upon cooling to ice-bath temperature. The crystals were collected and recrystallized from hot concentrated ammonia solution, washed first with absolute ethanol and then with anhydrous ether, and finally dried *in vacuo* at room temperature overnight. *Anal.* Calcd for $Pt(NH_3)_2(CN)_2$: C, 8.54; H, 2.15; N, 19.93; Pt, 69.38. Found: C, 8.52; H, 2.13; N, 20.05; Pt, 69.32. Ir: $\bar{\nu}_{CN}$ 2130 and 2145 $cm^{-1}$.

**Dicyano(ethylenediamine)platinum(II), Pt(en)$(CN)_2$.**[15] Platinum(II) cyanide[16] was heated with excess 20% aqueous ethylenediamine until all the solid dissolved. The solution was evaporated to dryness, and the residue was recrystallized from hot water. Cream-colored crystals were collected by suction filtration, washed first with absolute ethanol and then with anhydrous ether, and finally dried *in vacuo* at room temperature. *Anal.* Calcd for $Pt(CN)_2(H_2NCH_2CH_2NH_2)$: C, 15.65; H, 2.62; N, 18.24; Pt, 63.50. Found: C, 15.65; H, 2.56; N, 18.37; Pt, 63.37. Ir: $\bar{\nu}_{CN}$ 2132 and 2148 $cm^{-1}$.

**Dicyano(*l*-1,2-propanediamine)platinum(II), Pt(*l*-pn)$(CN)_2$.** A stoichiometric amount of platinum(II) cyanide was added to an aqueous solution of *l*-1,2-propanediamine dihydrochloride (Strem Chemicals, Inc.), which was made slightly basic with sodium hydroxide, and the resulting mixture was refluxed for 50 hr. Some insoluble matter was removed while the solution was still hot, and the volume of the filtrate was decreased to half by evaporating gently. Crystallization occurred on cooling the solution to ice-bath temperature. The white crystals were collected, washed first with absolute ethanol and then with anhydrous ether, and finally dried *in vacuo* at room temperature. *Anal.* Calcd for Pt(*l*-pn)$(CN)_2\cdot 0.33H_2O$: C, 18.35; H, 3.29; N, 17.12; Pt, 59.62. Found: C, 18.32; H, 3.33; N, 16.70; Pt, 59.73. Ir: $\bar{\nu}_{CN}$ 2150 $cm^{-1}$.

**Cyano(diethylenetriamine)platinum(II) Ion, Pt(dien)$CN^+$.** A concentrated aqueous solution of $[Pt(dien)Cl]ClO_4$, prepared from the chloride salt[17] by precipitation with concentrated perchloric acid at ice temperature, was treated with a stoichiometric amount of silver oxide dissolved in concentrated perchloric acid. After 30 min at boiling temperature, silver chloride was removed by filtration and the filtrate was gently evaporated to one-third of its original volume. A stoichiometric amount of potassium cyanide was added whereupon potassium perchlorate precipitated as the solution was cooled in an ice bath. Isolation of $[Pt(dien)CN]ClO_4$ as a solid was not possible due to its extremely high solubility in aqueous solution. Attempts to use absolute alcohol or acetone to lower the solubility of the perchlorate salt were not successful.

**Spectral Measurements.** All solutions for absorption and MCD spectra were prepared using spectral grade solvents. Solution absorption spectra were measured on a Cary 1501 spectrophotometer and MCD measurements were made with a Durrum-Jasco ORD/UV-5 (with CD attachment) equipped with a permanent magnet (field = 10.5 kG). The calibration of the CD instrument has been described previously.[18] Infrared measurements were made using a Beckman IR 12 spectrophotometer.

Low-temperature measurements were made using a Cryotip hydrogen refrigerator (Air Products and Chemicals, Inc.). Transparent poly(vinyl alcohol) (PVA) films were prepared as follows. The complex was dissolved in a 6% aqueous solution of PVA powder (Matheson Coleman and Bell, 99% hydrolyzed). The resulting mixture was heated on a water bath until all the PVA dissolved. The viscous solution was spread on a microscope slide and dried in air for 24 hr. The film was then peeled off carefully and allowed to dry at room temperature about 3 days. For low-temperature spectra the film was sandwiched between two indium plates and mounted in the Cryotip sample holder. The temperature below 100°K was measured with a gallium arsenide diode (TG-100 Cryogenic Sensor, Lake Shore Cryotronics, Inc.).

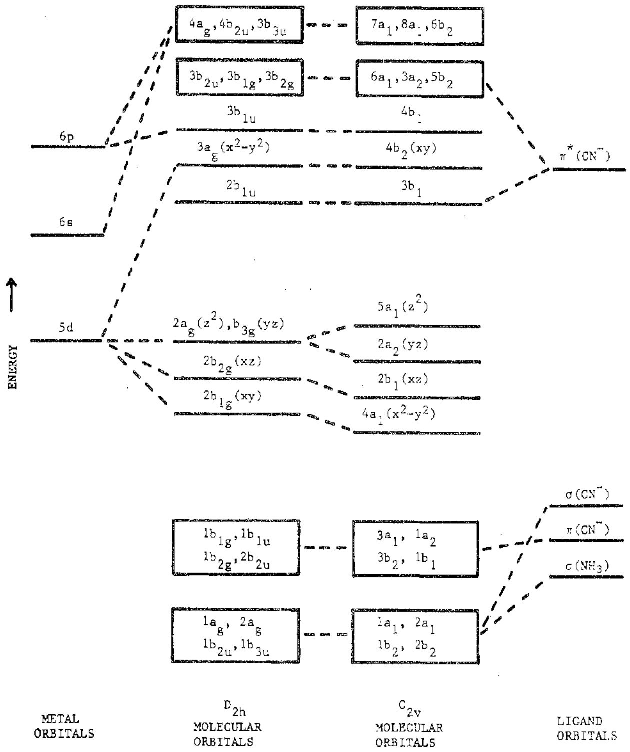

**Figure 1.** Molecular orbital energy levels for complexes of $D_{2h}$ symmetry and $C_{2v}$ symmetry.

## Results and Discussion

**Molecular Orbital Energy Levels and Excited States.** Energy level diagrams for $Pt(CN)_4^{2-}$ and $Pt(NH_3)_4^{2+}$ ($D_{4h}$) have been published previously, together with the symmetry representations of the excited states expected for the M → L and d → p transitions.[5,19] Each complex has a diamagnetic, nondegenerate ground state designated $^1A_{1g}$. The highest energy occupied orbitals are the d orbitals, and the lowest unoccupied orbital for $Pt(CN)_4^{2-}$ is designated $2a_{2u}$ and is based mainly on the $CN^-$ ligands.

For the lower symmetry cyanoamine complexes ($D_{2h}$ and $C_{2v}$) simplified one-electron molecular orbital energy level diagrams are sketched in Figure 1. The choice of coordinate system places the $CN^-$ ligands on the $x$ axis and the ammine ligands on the $y$ axis for *trans*-$Pt(NH_3)_2(CN)_2$, while for the $C_{2v}$ complexes, the $x$ axis was chosen to lie along the molecular symmetry axis, $C_2(x)$, and the $z$ axis to lie perpendicular to the molecular plane. The highest occupied orbitals of Figure 1 are designated $2a_g(z^2)$ and $b_{3g}(yz)$ for $D_{2h}$ and $5a_1(z^2)$ for $C_{2v}$; the complexes have diamagnetic, nondegenerate ground states designated $^1A_g$ and $^1A_1$, respectively. Table I presents the M → L excited configurations for the $D_{2h}$ and $C_{2v}$ complexes involving the lowest $\pi^*$ $CN^-$ level and the symmetry representations of the corresponding excited states. The double-group representations, appropriate for describing the spin–orbit states, are characterized by the lack of spin multiplicity superscripts.

The coordinates in $D_{4h}$ symmetry transform as $a_{2u}(z)$ and $e_u(x, y)$, while those in $D_{2h}$ transform as $b_{1u}(z)$, $b_{2u}(y)$, and $b_{3u}(x)$ and those in $C_{2v}$ as $a_1(x)$, $b_1(z)$, and $b_2(y)$. Therefore only electronic transitions to $^1A_{2u}$ and $^1E_u$ states in $D_{4h}$, $^1B_{1u}$, $^1B_{2u}$, and $^1B_{3u}$ states in $D_{2h}$, and $^1A_1$, $^1B_1$, and $^1B_2$ states in $C_{2v}$ are fully allowed by dipole selection rules. However, in the presence of spin–orbit coupling the spin multiplicity selection rules break down, and transitions to formally triplet

**Table I.** Excited Configurations and Symmetry Representations of Excited States

| Excited confign[a] | Excited states (no spin–orbit coupling) | Double-group states (spin–orbit coupling) |
|---|---|---|
| | $D_{2h}$ Symmetry | |
| $[2a_g(z^2)][2b_{1u}]$ | $^1B_{1u}$, $^3B_{1u}$ | $B_{1u}$, $A_u$, $B_{2u}$, $B_{3u}$ |
| $[b_{3g}(yz)][2b_{1u}]$ | $^1B_{2u}$, $^3B_{2u}$ | $B_{2u}$, $A_u$, $B_{1u}$, $B_{3u}$ |
| $[2b_{2g}(xz)][2b_{1u}]$ | $^1B_{3u}$, $^3B_{3u}$ | $B_{3u}$, $A_u$, $B_{1u}$, $B_{2u}$ |
| $[2b_{1g}(xy)][2b_{1u}]$ | $^1A_u$, $^3A_u$ | $A_u$, $B_{1u}$, $B_{2u}$, $B_{3u}$ |
| | $C_{2v}$ Symmetry | |
| $[5a_1(z^2)][3b_1]$ | $a^1B_1$, $a^3B_1$ | $B_1$, $A_1$, $A_2$, $B_2$ |
| $[2a_2(yz)][3b_1]$ | $^1B_2$, $^3B_2$ | $B_2$, $A_1$, $A_2$, $B_1$ |
| $[2b_1(xz)][3b_1]$ | $^1A_1$, $^3A_1$ | $A_1$, $A_2$, $B_1$, $B_2$ |
| $[4a_1(x^2-y^2)][3b_1]$ | $b^1B_1$, $b^3B_1$ | $B_1$, $A_1$, $A_2$, $B_2$ |

[a] Filled levels omitted; see Figure 1.

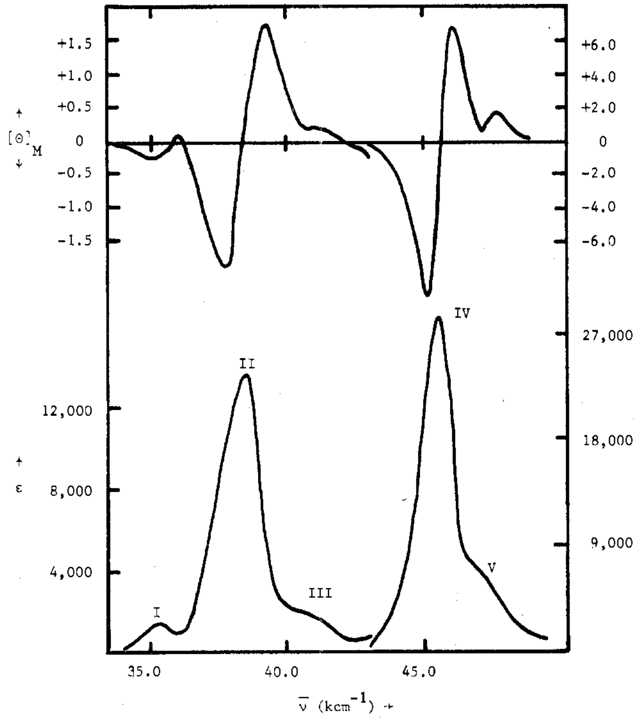

**Figure 2.** Absorption (lower curves) and MCD (upper curves) spectra of $[(n\text{-}C_4H_9)_4N]_2[Pt(CN)_4]$ in acetonitrile.

excited states may gain appreciable intensity by admixtures of singlet states.

**Electronic Absorption and MCD Spectra.** Electronic absorption and MCD spectra for $Pt(CN)_4^{2-}$ and $Pt(NH_3)_4^{2+}$ in aqueous solution have been reported previously.[5,6,19] Figure 2 presents absorption and MCD spectra for $Pt(CN)_4^{2-}$ in acetonitrile solution. With the exception of a shoulder resolved at 47.0 kK on the high-energy side of the 45.5-kK band, the acetonitrile spectra agree substantially with that reported for aqueous solution. The 47.0-kK shoulder, which has a distinctly resolved positive maximum at 47.44 kK in the MCD, has not been reported previously. The maximum in the MCD appears to be the positive lobe of a positive *A* term centered at ~46.9 kK, the negative lobe of which is obscured by overlapping with the strong positive *A* term at 45.5 kK.

Aqueous absorption and MCD spectra for *trans*-$Pt(NH_3)_2(CN)_2$ and $Pt(en)(CN)_2$ are given in Figures 3 and 4. Both the absorption and MCD spectra show that the cyanoamine complexes exhibit intense charge-transfer bands which have a pattern similar to those of $Pt(CN)_4^{2-}$, but which are shifted to slightly higher energies. The apparent *A* term associated with band II in the MCD spectra for *trans*-$Pt(NH_3)_2(CN)_2$ is particularly striking. It should be pointed out that only *B* terms are expected for the $D_{2h}$ and $C_{2v}$ complexes because there are no strictly degenerate excited states. However two overlapping *B* terms of opposite signs arising from adjacent excited states, which are close in energy and connected by a magnetic moment, will give the appearance of an *A* term. Such "pseudo *A*" terms have been discussed[6] in connection with the MCD of $Pt(CN)_4^{2-}$. Thus, the MCD in the region of band II for *trans*-$Pt(NH_3)_2(CN)_2$, and band II for $Pt(en)(CN)_2$ also, is ascribed to a pseudo *A* term.

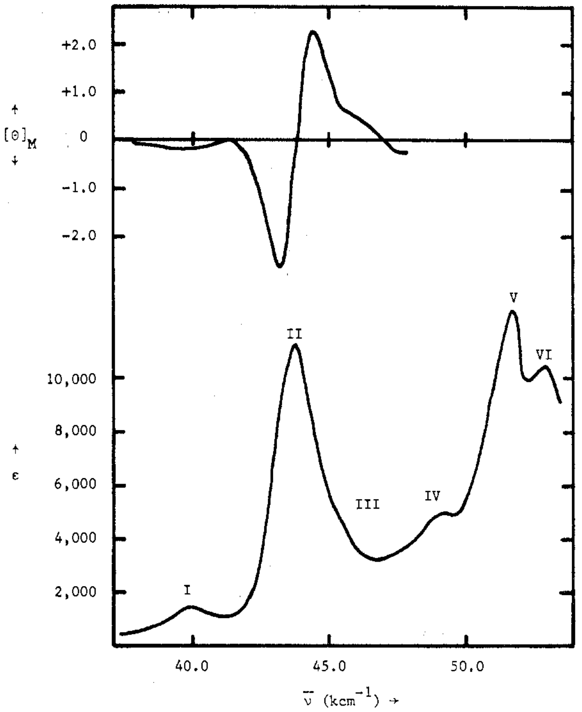

**Figure 3.** Absorption (lower curve) and MCD (upper curve) spectra of *trans*-$Pt(NH_3)_2(CN)_2$ in $H_2O$.

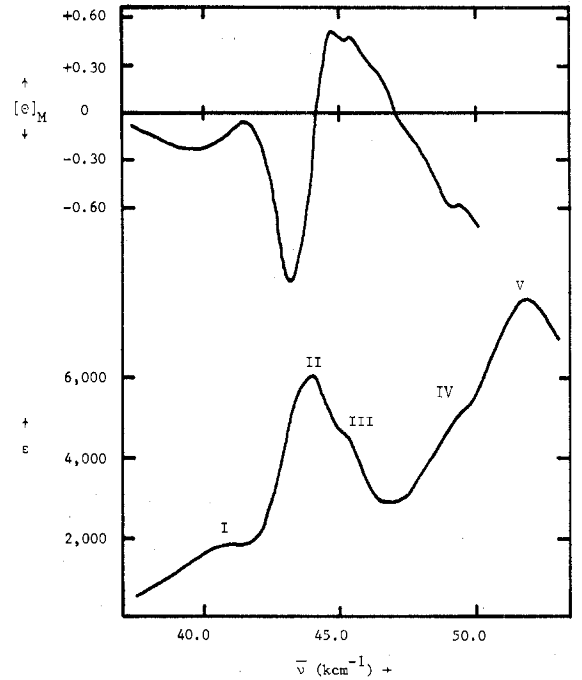

**Figure 4.** Absorption (lower curve) and MCD (upper curve) spectra of $Pt(en)(CN)_2$ in $H_2O$.

The low-temperature absorption spectral measurements on $Pt(CN)_4^{2-}$, *trans*-$Pt(NH_3)_2(CN)_2$, and $Pt(en)(CN)_2$ in PVA polymer films show improved resolution over the room-temperature measurements; spectra for *trans*-$Pt(NH_3)_2(CN)_2$,

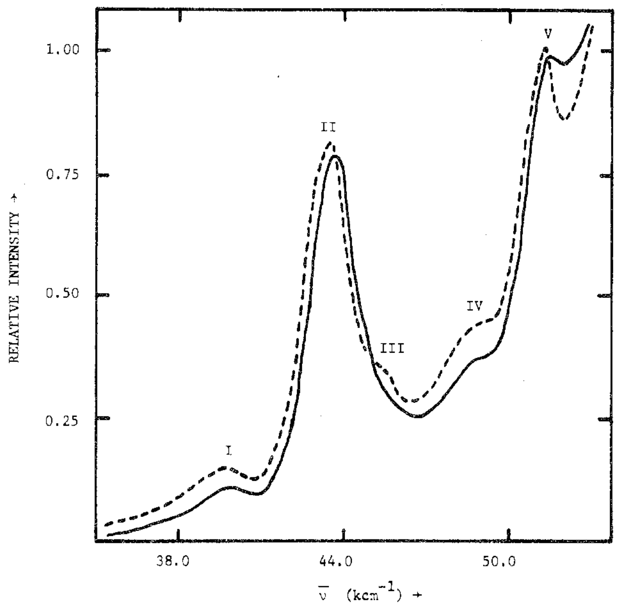

**Figure 5.** Absorption spectra of *trans*-$Pt(NH_3)_2(CN)_2$ in a PVA film: ——, 300°K; - - -, 26°K.

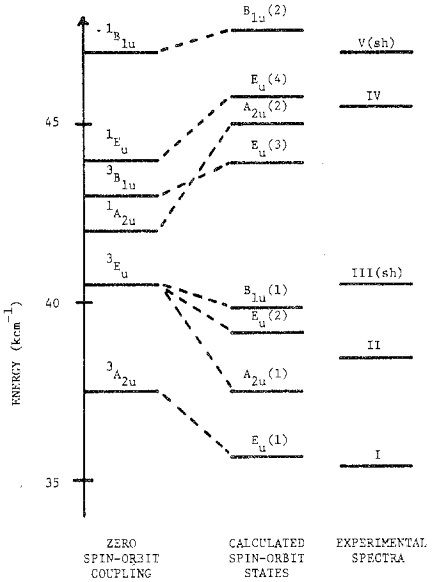

**Figure 6.** Spin-orbit states for $Pt(CN)_4{}^{2-}$. Input parameters for the calculated states (in kK): $\zeta = 3.0$; $^1B_{1u}$, 47.0; $^3B_{1u}$ 43.0; $^1E_u$, 43.5; $^3E_u$, 40.5; $^1A_{2u}$, 42.0; $^3A_{2u}$, 37.5. Experimental absorption spectral data for acetonitrile solution.

which are typical of the low-temperature results, are shown in Figure 5. Detailed spectral data for these and other measurements are collected in Table II.

**Calculation of Spin-Orbit States.** The approach taken to treating spin-orbit interaction in the M → L excited states is basically the same as described by Piepho, *et al.*[6] The spin-orbit interaction in the excited configurations (Table I) was treated as a perturbation on the singlet and triplet M → L excited states which would be assumed in the absence of strong coupling. Input data included estimated energies for the unperturbed states and a value of the spin-orbit parameter $\zeta$. Appropriate secular determinants were diagonalized to find the energies of the spin-orbit states, which were then compared with experimental spectra. The spin-orbit Hermitian secular determinants are tabulated in Table III. The spin-orbit matrix elements were calculated by approximating the molecular orbitals derived from the metal d orbitals as metal d functions. The spin-orbit matrix elements then reduce to matrix elements of angular momentum between the d orbitals. Calculated energies of the spin-orbit states are plotted along with the experimental spectra in Figures 6-8; eigenvalues and the mixing coefficients are included in Table IV.[20] Successful input parameters are given in Figures 6-8. In each case, a wide range of parameters was tried, but values of $\zeta$ and energies of the singlet and triplet unperturbed states significantly different from those given in Figures 6-8 failed to give a favorable fit to the absorption spectra and give states which were consistent with the MCD spectra.

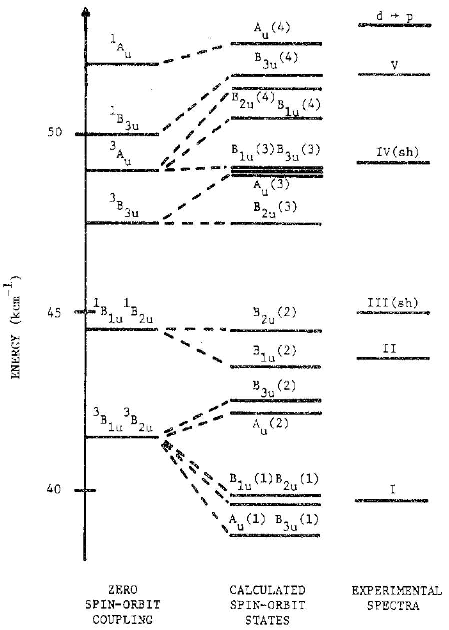

**Figure 7.** Spin-orbit states for *trans*-$Pt(NH_3)_2(CN)_2$. Input parameters for the calculated states (in kK): $\zeta = 3.0$; $^1A_u$, 52.0; $^3A_u$, 49.0; $^1B_{3u}$, 50.0; $^3B_{3u}$, 47.5; $^1B_{1u}$, 45.0; $^3B_{1u}$, 41.5; $^1B_{2u}$, 45.0; $^3B_{2u}$, 41.5. Experimental absorption spectral data for $H_2O$ solution.

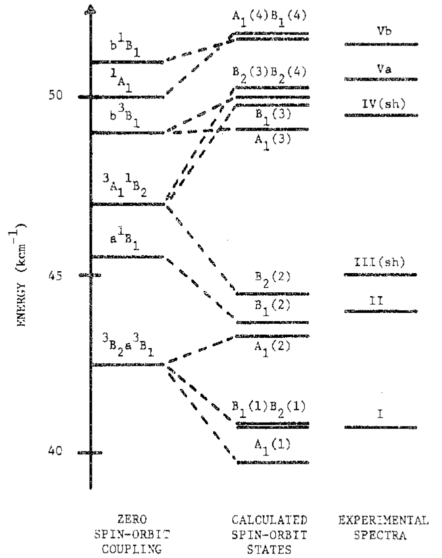

**Figure 8.** Spin-orbit states for $Pt(en)(CN)_2$. Input parameters for the calculated states (in kK): $\zeta = 3.0$; $b^1B_1$, 51.0; $b^3B_1$, 49.0; $^1A_1$, 50.0; $^3A_1$, 47.0; $^1B_2$, 47.0; $^3B_2$, 42.5; $a^1B_1$, 45.5; $a^3B_1$, 42.5. Experimental absorption spectral data for $H_2O$ solution except band V, which is from data for a PVA film at 26°K.

**Spectral Assignments.** The intense charge-transfer bands in the absorption spectrum of $Pt(CN)_4{}^{2-}$ have been assigned to M → L transitions,[3-6] and this assignment has been generally accepted, though there has not been uniform agreement as to specific, detailed band assignments as noted earlier. Ligand field transitions are expected to be above 50

**Table II.** Spectral Data and Band Assignments

| Band | $\bar{\nu}$, ($\epsilon$), kK ($M^{-1}$ cm$^{-1}$) ($H_2O$, 300°K) | $\bar{\nu}$ (rel abs), kK (PVA, 26°K) | Obsd MCD term | Excited-state Assignmt |
|---|---|---|---|---|
| | | $Pt(CN)_4^{2-}$ [a] | | |
| I | 35.40 (1230) | 35.80 (0.10) | $+B$, $+A$ | $E_u(1)$ |
| II | 38.45 (12,900) | 38.50 (0.43)[b] | $+A$, $+A$[c] | $A_{2u}(1)$, $E_u(2)$ |
| | | 39.40 (0.49) | | |
| III | 40.50 (1840)[b] | 41.50 (0.12) | $-B$ | $E_u(2) + \nu_{CN}$ |
| IV | 45.50 (29,300) | 46.10 (1.00) | $+A$, $+A$[c] | $A_{2u}(2)$, $E_u(4)$ |
| V | 47.00 (8780)[b] | | $+A$ | $E_u(4) + \nu_{CN}$ |
| | | *trans*-$Pt(NH_3)_2(CN)_2$ | | |
| I | 39.80 (1380) | 39.80 (0.16) | $+B$ | $B_{1u}(1)$, $B_{2u}(1)$ |
| II | 43.75 (10,800) | 43.35 (0.82) | $+A$[c] | $B_{1u}(2)$, $B_{2u}(2)$ |
| III | 45.00 (5000)[b] | 45.00 (0.38)[b] | $-B$ | $B_{1u}(2) + \nu_{CN}$ or $B_{2u}(2) + \nu_{CN}$ |
| IV | 49.25 (4800)[b] | 49.00 (0.45)[b] | | $B_{1u}(3)$, $B_{3u}(3)$ |
| V | 51.75 (13,000) | 51.25 (1.00) | | $B_{3u}(4)$ |
| VI | 53.15 (10,500) | | | $^1B_{1u}$, $^1B_{2u}$ (d → p) |
| | | Pt(en)$(CN)_2$ | | |
| I | 40.75 (1800) | 40.80 (0.29) | $+B$ | $B_1(1)$, $B_2(1)$ |
| II | 44.00 (6000) | 43.80 (0.76) | $+A$[c] | $B_1(2)$, $A_1(2)$ |
| III | 45.00 (4700)[b] | 45.00 (0.57)[b] | $-B$ | $B_2(2)$ |
| IV | 49.50 (5150)[b] | 49.00 (0.94)[b] | $+B$ | $B_1(3)$ |
| V | 52.00 (7800) | 50.50 (0.96) | | $B_2(3)$, $B_2(4)$ |
| | | 51.50 (1.00) | | $A_1(4)$, $B_1(4)$ |

| Band | $\bar{\nu}$ ($\epsilon$), kK ($M^{-1}$ cm$^{-1}$) ($H_2O$, 300°K) | Obsd MCD term | Excited-state assgnmt | Band | $\bar{\nu}$ ($\epsilon$), kK ($M^{-1}$ cm$^{-1}$) ($H_2O$, 300°K) | Obsd MCD term | Excited-state assignmt |
|---|---|---|---|---|---|---|---|
| | Pt($l$-pn)$(CN)_2$ | | | | Pt(dien)$(CN)^+$ [d] | | |
| I | 41.00 (1800) | $+B$ | $B_1(1)$, $B_2(1)$ | I | 43.00 (0.43)[b] | | $A_1$, $B_1$, $B_2$ ($^3B_1$, $^3B_2$) |
| II | 44.00 (5800) | $+A$[c] | $A_1(2)$, $B_1(2)$ | II | 45.75 (1.55) | | $B_1$, $B_2$ ($^1B_1$, $^1B_2$) |
| III | 45.50 (4050)[b] | $-B$ | $B_2(2)$ | III | 47.80 (1.70) | | $A_1$ ($^1A_1$) |
| IV | 49.50 (4700)[b] | $+B$ | $B_1(3)$ | IV | 49.00 (1.56)[b] | | $A_2$(?) |
| V | 51.75 (7650) | | $A_1(4)$, $B_1(4)$ | V | 54.00 (2.0) | | $^1B_1$, $^1B_2$ (d → p) |
| | *cis*-$Pt(NH_3)_2(CN)_2$ | | | | $Pt(NH_3)_4^{2+}$ [e] | | |
| I | 40.85 (2060) | $+B$ | $B_1(1)$, $B_2(1)$ | I | 34.75 (40) | $+B$ | $^3A_{2g}$, $^3E_g$ |
| II | 44.20 (4550) | $+B$, $-B$ | $B_1(2)$, $A_1(2)$ | II | 41.50 (133)[b] | $-B$ | $^1A_{2g}$, $^1E_g$ |
| III | 46.50 (5300) | $+B$ | $B_2(2)$ | III | 45.50 (563)[b] | $+B$ | $^1B_{1g}$ |
| IV | 48.00 (5850) | $+B$ | $B_1(3)$ | IV | 50.95 (10,600) | $+A$ | $^1E_u$ (d → p) |
| V | 52.00 (6680) | | $A_1(4)$, $B_1(4)$ | | | | |

[a] Solution spectra obtained from $(n\text{-}C_4H_9)_4N^+$ salt in acetonitrile; PVA film prepared from $H_2O$ solution of potassium salt. [b] Shoulder. [c] Pseudo $A$ term—see text. [d] Numbers in parentheses are relative absorbance; see footnote 22. [e] Assignments from ref 5 and 19.

kK.[5] In the $Pt(NH_3)_4^{2+}$ spectrum an intense band at 50.95 kK has been assigned as a d → p transition.[5,19] Lower energy bands are much weaker and have been assigned as ligand field bands.[5] Therefore in the cyanoamine complexes, both M → L and d → p transitions might be anticipated; ligand field bands are expected to be at higher energy than for $Pt(NH_3)_4^{2+}$ and therefore obscured by the intense absorptions. Detailed spectral assignments for each complex are included in Table II. These assignments will be briefly discussed, each in turn.

**$Pt(CN)_4^{2-}$.** Calculated spin–orbit states for the $Pt(CN)_4^{2-}$ ion are shown in Figure 6. These results are in substantial agreement with those of Piepho, *et al.*,[6] and indicate that the M → L transitions can be satisfactorily explained by excitations from the occupied d orbitals to only the $2a_{2u}$ $\pi^*$ $CN^-$ orbital. Reasonable values of $\zeta_{5d}$ distribute excited states over 9–12 kK of energy, comparable to the observed energy span in the experimental spectra. In fact, attempts to include the second lowest lying $\pi^*$ $CN^-$ orbital, $3e_u$, in excited configurations as suggested by previous workers,[3-5] required an unreasonably small $\zeta_{5d}$ parameter (<1 kK).

The lowest energy absorption for $Pt(CN)_4^{2-}$, band I, is assigned to $E_u(1)$ which is mainly derived from $^3A_{2u}$. Associated with this band, the MCD shows a positive $A$ term (though it is unsymmetrical due to the presence of a relatively large positive $B$ term at the same energy). As pointed out by Piepho, *et al.*,[6] the *sign* of the $A$ term expected for the transition to $E_u(1)$, and to all other $E_u(i)$ states, can be calculated by approximating the $2a_{2u}$ $\pi^*$ $CN^-$ orbital as a carbon 2p function and the metal orbitals as 5d functions and including only one-centered integrals; the approximate expression is given in eq 1, where $\beta$ is the Bohr magneton, $D(^1E_u)$ is the dipole

$$A \cong {}^1\!/_2\beta[-2|a_i|^2 + 2|b_i|^2 + |c_i|^2 + |d_i|^2]|d_i|^2D(^1E_u) \quad (1)$$

strength of the fully allowed $^1A_{1g} \rightarrow {}^1E_u$ transition, and $a_i$, $b_i$, $c_i$, and $d_i$ are coefficients of $^3B_{1u}$, $^3A_{2u}$, $^3E_u$, and $^1E_u$, respectively, in the $E_u(i)$ eigenvectors (Table IV[20]). From the magnitudes of the coefficients, the $A$ term for $E_u(1)$ is expected to be positive, in agreement with experiment. The previous assignment[5] of band I as a transition to the symmetry-forbidden $^1B_{1u}$ state or to the $E_u(^3B_{1u})$ state must be discarded because the observation of the $A$ term excludes the former and the *sign* of the $A$ term observed (positive) excludes the latter; the $A$ term predicted for $E_u(^3B_{1u})$ is expected to be *negative*.

The envelope of band II is known to cover at least two transitions. Resolution of these transitions has been achieved in the low-temperature (26°K) PVA spectra reported here and also in the low-temperature (77°K) EPA measurements reported previously.[5] The spin–orbit calculations place the $A_{2u}(1)$ and $E_u(2)$ states in this energy region, and the $A$ term for $E_u(2)$ is calculated to be positive, consistent with the observed MCD. However, $A_{2u}(i)$ and $E_u(j)$ states are connected by a magnetic moment in the presence of a magnetic field, and thus the possibility of a pseudo $A$ term for band II may be visualized. From a calculation of the signs of the $\langle A_{2u}(1)|\mu|E_u(2)\rangle$ matrix element ($\mu$ is the magnetic moment operator) and the overall $B$ terms involved, the pseudo $A$ term

**Table III.** Spin-Orbit Secular Determinants (Upper Triangles)[a]

$D_{4h}$ Symmetry

$$\mathrm{E_u}\qquad \begin{vmatrix} ^3\mathrm{B_{1u}}-E & 0 & i\zeta/2 & -\zeta/2 \\ & ^3\mathrm{A_{2u}}-E & -i3^{1/2}\zeta/2 & -3^{1/2}\zeta/2 \\ & & ^3\mathrm{E_u}-E & -i\zeta/2 \\ & & & ^1\mathrm{E_u}-E \end{vmatrix}$$

$$\mathrm{A_{2u}}\qquad \begin{vmatrix} ^1\mathrm{A_{2u}}-E & -3^{1/2}\zeta/2 \\ & ^3E_{\mathrm{u}}-E \end{vmatrix}$$

$$\mathrm{B_{1u}}\qquad \begin{vmatrix} ^1\mathrm{B_{1u}}-E & 2^{1/2}\zeta/2 \\ & ^3\mathrm{E_u}-E \end{vmatrix}$$

$D_{2h}$ Symmetry

$$\mathrm{B_{1u}}\qquad \begin{vmatrix} ^3\mathrm{A_u}-E & 0 & i\zeta/2 & i\zeta/2 \\ & ^1\mathrm{B_{1u}}-E & 3^{1/2}\zeta/2 & -3^{1/2}\zeta/2 \\ & & ^3\mathrm{B_{3u}}-E & -\zeta/2 \\ & & & ^3\mathrm{B_{2u}}-E \end{vmatrix}$$

$$\mathrm{B_{2u}}\qquad \begin{vmatrix} ^3\mathrm{A_u}-E & 0 & i\zeta/2 & -\zeta/2 \\ & ^3\mathrm{B_{1u}}-E & -i3^{1/2}\zeta/2 & 3^{1/2}\zeta/2 \\ & & ^3\mathrm{B_{3u}}-E & i\zeta/2 \\ & & & ^1\mathrm{B_{2u}}-E \end{vmatrix}$$

$$\mathrm{B_{3u}}\qquad \begin{vmatrix} ^3\mathrm{A_u}-E & 0 & -\zeta/2 & i\zeta/2 \\ & ^3\mathrm{B_{1u}}-E & -3^{1/2}\zeta/2 & -i3^{1/2}\zeta/2 \\ & & ^1\mathrm{B_{3u}}-E & i\zeta/2 \\ & & & ^3\mathrm{B_{2u}}-E \end{vmatrix}$$

$$\mathrm{A_u}\qquad \begin{vmatrix} ^1\mathrm{A_u}-E & 0 & \zeta/2 & -\zeta/2 \\ & ^3\mathrm{B_{1u}}-E & -i3^{1/2}\zeta/2 & -i3^{1/2}\zeta/2 \\ & & ^3\mathrm{B_{3u}}-E & \zeta/2 \\ & & & ^3\mathrm{B_{2u}}-E \end{vmatrix}$$

$C_{2v}$ Symmetry

$$\mathrm{A_1}\qquad \begin{vmatrix} \mathrm{b}\,^3\mathrm{B_1}-E & \zeta/2 & -i\zeta/2 & 0 \\ & ^1\mathrm{A_1}-E & i\zeta/2 & -3^{1/2}\zeta/2 \\ & & ^3\mathrm{B_2}-E & i3^{1/2}\zeta/2 \\ & & & \mathrm{a}\,^3\mathrm{B_1}-E \end{vmatrix}$$

$$\mathrm{B_1}\qquad \begin{vmatrix} \mathrm{b}\,^1\mathrm{B_1}-E & -\zeta/2 & -\zeta/2 & 0 \\ & ^3\mathrm{A_1}-E & -\zeta/2 & 3^{1/2}\zeta/2 \\ & & ^3\mathrm{B_2}-E & -3^{1/2}\zeta/2 \\ & & & \mathrm{a}\,^1\mathrm{B_1}-E \end{vmatrix}$$

$$\mathrm{B_2}\qquad \begin{vmatrix} \mathrm{b}\,^3\mathrm{B_1}-E & i\zeta/2 & \zeta/2 & 0 \\ & ^3\mathrm{A_1}-E & i\zeta/2 & i3^{1/2}\zeta/2 \\ & & ^1\mathrm{B_2}-E & 3^{1/2}\zeta/2 \\ & & & \mathrm{a}\,^3\mathrm{B_1}-E \end{vmatrix}$$

[a] The determinant elements are phase dependent, and although the choice of phase is arbitrary, one must take care to be internally consistent. Thus although some of the elements of the $\mathrm{E_u}$ determinant for $D_{4h}$ symmetry given here differ in phase from those given in ref 6, the determinants are *equivalent* and yield identical eigenvalues for the same input parameters.

is expected to be positive and therefore reinforce the positive *A* term of $\mathrm{E_u}(2)$.[6] A similar situation is envisioned for band IV. The $\mathrm{A_{2u}}(2)$ and $\mathrm{E_u}(4)$ states are calculated to be close in energy and are both expected to lie under the 45.5-kK band. The *A* term for $\mathrm{E_u}(4)$ and the pseudo *A* term for the $\mathrm{A_{2u}}(2)$ interaction with $\mathrm{E_u}(4)$ are predicted to be positive, consistent with the experimental MCD. In view of the approximations involved in eq 1, the magnitudes of the calculated *A* and pseudo *A* terms are considered less reliable than the overall sign. For both bands II and IV a detailed calculation using accurate wave functions for the molecular orbitals would be required in order to give reliable estimates of the *A* and pseudo *A* contributions to the MCD.

The weak shoulder at 40.5 kK, band III, and the shoulder at 47.0 kK, band V, are not accounted for by the $\mathrm{A_{2u}}$ and $\mathrm{E_u}$ spin-orbit states. Their positions ~1500–2000 cm$^{-1}$ higher in energy than bands II and IV and their lower intensity compared to these intense bands suggest excited-state vibrational excitations of the CN$^-$ ligand built on $\mathrm{E_u}(2)$ and $\mathrm{E_u}(4)$ (the ground-state $\bar{\nu}_{\mathrm{CN}}(\mathrm{a_{1g}})$ determined from Raman measurements is 2168 cm$^{-1}$ [21]). If bands III and V are members of totally symmetric vibrational progressions on the $\mathrm{E_u}$ transitions, then *A* terms of the same sign as these transitions are expected in the MCD. The MCD in the region of band V is consistent with this assignment; the MCD in the region of band II, however, is less clear. The assignment of bands III and V as ligand field transitions is considered unlikely since the lowest energy d → d transition in $\mathrm{Pt(CN)_4}^{2-}$ is expected to be above 50 kK.[5]

***trans*-$\mathbf{Pt(NH_3)_2(CN)_2}$.** Calculated spin-orbit states for *trans*-$\mathrm{Pt(NH_3)_2(CN)_2}$ are given in Figure 7. The lowest energy band, band I, is assigned to the states $\mathrm{B_{1u}}(1)$ and $\mathrm{B_{2u}}(1)$, which are derived mainly from $^3\mathrm{B_{2u}}$ and $^3\mathrm{B_{1u}}$, respectively. Two states, $\mathrm{B_{3u}}(1)$ and $\mathrm{A_u}(1)$, are calculated to lie at lower energy (both at 38.8 kK), but both states have negligible singlet character and hence transitions to them should be very weak. The MCD in the region of band I reveals only a broad positive *B* term. Though not terribly informative, it is not inconsistent with our assignment.

The spin-orbit calculations place $\mathrm{B_{1u}}(2)$ and $\mathrm{B_{2u}}(2)$ in the region of band II. As noted above the MCD shows a positive pseudo *A* term for band II. From a calculation of the signs of matrix elements $\langle \mathrm{B_{1u}}|\mu|\mathrm{B_{2u}}\rangle$, assuming that the largest contribution to the pseudo *A* term arises from *B* terms of adjacent states, the pseudo *A* term for band II is predicted to be positive, in good agreement with experiment. Furthermore, both $\mathrm{B_{1u}}(2)$ and $\mathrm{B_{2u}}(2)$ are expected to have substantial singlet character (48% $^1\mathrm{B_{1u}}$ and 64% $^1\mathrm{B_{2u}}$, respectively), which is consistent with the observed intensity of band II.

Band IV is assigned to $\mathrm{B_{1u}}(3)$ and $\mathrm{B_{3u}}(3)$ and band V to $\mathrm{B_{3u}}(4)$, on the basis of the calculated energies of these states. The singlet character of these states parallels the observed intensities of bands IV and V (singlet character of $\mathrm{B_{1u}}(3)$, $\mathrm{B_{3u}}(3)$, and $\mathrm{B_{3u}}(4)$ is 18% $^1\mathrm{B_{1u}}$, 9% $^1\mathrm{B_{3u}}$, and 75% $^1\mathrm{B_{3u}}$, respectively).

Band III, which is resolved in the low-temperature PVA spectra (Figure 5), is not accounted for by the spin-orbit model. By analogy to band III in the $\mathrm{Pt(CN)_4}^{2-}$ spectrum, this band is assigned as a vibrational excitation of CN$^-$ built on $\mathrm{B_{1u}}(2)$ or $\mathrm{B_{2u}}(2)$. However an alternate possibility for band III which cannot be excluded is a spin-allowed ligand field transition, since the $\mathrm{Pt(NH_3)_4}^{2+}$ complex exhibits spin-allowed transitions in this energy region at 41.5 and 45.5 kK. Band VI is also not accounted for by the spin-orbit model. Since the intensity is appropriate for an allowed transition, band VI is assigned as the d → p excitation $^1\mathrm{A_g} \rightarrow {}^1\mathrm{B_{1u}}, {}^1\mathrm{B_{2u}}$ [$2\mathrm{a_g}(z^2)$, $2\mathrm{b_{3g}}(yz) \rightarrow 3\mathrm{b_{1u}}$]. Such an assignment is not unreasonable since a d → p transition is observed for $\mathrm{Pt(NH_3)_4}^{2+}$ at similar energy.

***cis*-$\mathbf{Pt(NH_3)_2(CN)_2}$, Pt(en)(CN)$_2$, and Pt(*l*-pn)(CN)$_2$.** The absorption spectrum of *cis*-$\mathrm{Pt(NH_3)_2(CN)_2}$ was not as well resolved as those of the two chelate complexes. It is possible that the poor-quality spectrum was due to a small amount of the $[Pt(NH_3)_4][Pt(CN)_4]$ double complex salt in the sample as an impurity. This double complex salt would have the same elemental analysis as the cis complex, but the $Pt(CN)_4^{2-}$ absorptions are quite intense and even a small amount of this ion present as an impurity could alter the appearance of the absorption spectrum. The chelate complexes, however, gave well-resolved spectra which were quite similar. Therefore detailed spectral analysis and spin–orbit calculations were performed for the $Pt(en)(CN)_2$ data. The assignments of the spectra of *cis*-$Pt(NH_3)_2(CN)_2$ and $Pt(l\text{-pn})(CN)_2$ were then made by analogy with $Pt(en)(CN)_2$.

Calculated spin–orbit states for $Pt(en)(CN)_2$ are shown in Figure 8. Band I in the $Pt(en)(CN)_2$ spectrum is assigned as $B_1(1)$ and $B_2(1)$, which are mainly derived from $^3B_2$ and $a^3B_1$. The $A_1(1)$ state is calculated to be at lower energy (39.7 kK), but this state has very little singlet character (<1%), and thus a transition to this state would be very weak. Band II is assigned to $A_1(2)$ and $B_1(2)$; this assignment is expected to give rise to a pseudo *A* term since these states are quite close in energy. This expectation is borne out in the experimental MCD. Band III could be assigned as a $CN^-$ vibration built on $A_1(2)$ or $B_1(2)$, analogous to the assignment of band III in *trans*-$Pt(NH_3)_2(CN)_2$, but the band is much more distinct and has a higher relative intensity compared to band II than in the case of band III in the trans complex. The $B_2(2)$ state, which has 41% $^1B_2$ character, is placed by the calculation near the energy of band III. Therefore a transition to this state is a more reasonable assignment.

Bands IV and V were assigned on the basis of the spin–orbit calculations. It should be pointed out that the transition $d_{x^2-y^2} \rightarrow 3b_1$ is symmetry allowed for the $C_{2v}$ complexes. In contrast, the corresponding transitions for $Pt(CN)_4^{2-}$ and *trans*-$Pt(NH_3)_2(CN)_2$ ($d_{xy} \rightarrow 2a_{2u}$ and $d_{xy} \rightarrow 2b_{1u}$, respectively) are forbidden. Therefore an additional intense band might be anticipated in this energy region for the $C_{2v}$ complexes. Indeed, band V was resolved into two components at low temperature. Consequently the higher energy component is assigned as a transition to $A_1(4)$ and $B_1(4)$, the latter state arising from the $d_{x^2-y^2} \rightarrow 3b_1$ excitation. However a d → p assignment of one of the components of band V cannot be excluded entirely, but it is likely that a d → p transition for $Pt(en)(CN)_2$ would be at nearly the same energy as for *trans*-$Pt(NH_3)_2(CN)_2$ since the acceptor $6p_z$ orbital on the platinum interacts with the same number of ligands in both cases.

**$Pt(dien)(CN)^+$.** Although a solid salt of this complex was not isolated, stoichiometrically prepared solutions exhibited absorption bands which are entirely consistent with the formulation of the complex. The bands may be assigned by analogy to the other cyanoamine complexes.[22] Band I is assigned to states arising from the formally spin-forbidden $^3B_1$ and $^3B_2$ states associated with the $a_1(z^2) \rightarrow 3b_1$ and $a_2(yz) \rightarrow 3b_1$ transitions, respectively, while band II is assigned to the corresponding singlets, $^1B_1$ and $^1B_2$. Band III is assigned to the $^1A_1$ state associated with the $b_1(xz) \rightarrow 3b_1$ transition. Band IV is quite weak, appears as a very indistinct shoulder on band III, and may be the orbitally forbidden $^1A_2$ arising from $b_2(xy) \rightarrow 3b_1$. Finally band V is assigned to the d → p transitions $^1A_1 \rightarrow {^1B_1}, {^1B_2}$ $[a_1(z^2), a_2(yz) \rightarrow 4b_1]$.

**Bonding and Electronic Structure in $Pt(CN)_4^{2-}$ and the Cyanoamine Complexes.** It is encouraging that the simple spin–orbit model of Piepho, *et al.*,[6] involving only a single $\pi^*$ $CN^-$ acceptor level for excited configurations, works as well as it does in distributing excited states which are consistent with experimental absorption and MCD spectra. However, a comment on the successful input parameters used for the spin–orbit calculations is appropriate. First of all, the value of the platinum spin–orbit coupling constant used in the computations (3000 $cm^{-1}$) is 74% of the free ion constant of 4050 $cm^{-1}$,[23] indicating a modest reduction in $\zeta_{5d}$ in the complexes. Attempts to use significantly larger or smaller values of $\zeta_{5d}$ did not produce satisfactory fits to the experimental spectra. This reduction of $\zeta_{5d}$ from the free-ion value is not surprising since both $CN^-$ and $NH_3$ ligands are good $\sigma$ donors. The spin–orbit coupling is proportional to the effective charge felt by the 5d electrons,[24] and $\sigma$ bonding to the metal 6s, $6p_x$, and $6p_y$ orbitals is expected to decrease the effective charge by core penetration and effective screening of the 5d electrons. Second, the energy differences between the singlet and triplet excited states of the same configuration indicated by the successful input parameters range from 3 to 5 kK. These differences seem too large in view of the spatial difference between the occupied (metal) and empty (ligand) orbitals involved in the M → L transitions. However, attempts to fit the spectra using smaller differences were unsuccessful. There is no satisfactory explanation of these differences at the present.

Since the M → L charge-transfer spectra in $Pt(CN)_4^{2-}$ and the cyanoamine complexes involve a single $\pi^*$ $CN^-$ orbital, the similarity in the pattern of absorption bands for these complexes must indicate a similarity in the ordering of the occupied metal d orbitals. The ordering of the occupied d orbitals, which can be obtained from the order of the excited states in the assigned spectra if differences in electronic repulsions in these states are assumed to be small, indicates the order $d_{z^2} > d_{xz}d_{yz} > d_{xy}$ for $Pt(CN)_4^{2-}$, the order $d_{z^2} \sim d_{yz} > d_{xz} > d_{xy}$ for *trans*-$Pt(NH_3)_2(CN)_2$, and the order $d_{z^2} \gtrsim d_{yz} > d_{xz} \gtrsim d_{x^2-y^2}$ for $Pt(en)(CN)_2$, $Pt(l\text{-pn})(CN)_2$, and *cis*-$Pt(NH_3)_2(CN)_2$ ($d_{z^2} \gtrsim d_{yz} > d_{xz} \gtrsim d_{xy}$ for $Pt(dien)(CN)^+$). The $d_{z^2}$ orbital is the highest occupied molecular orbital (HOMO) for each complex, though the $d_{yz}$ level in the cyanoamine complexes is found to be at very nearly the same energy, and small differences in electronic repulsions could alter the order of these two levels. The $d_\pi$ levels ($d_{yz}$, $d_{xz}$, and $d_{xy}$, or $d_{x^2-y^2}$ in $Pt(dien)(CN)^+$) are lower in energy than $d_{z^2}$, and the degeneracy of $d_{xz}$ and $d_{yz}$ in $Pt(CN)_4^{2-}$ is removed in the lower symmetry complexes.

In the case of *trans*-$Pt(NH_3)_2(CN)_2$, the $d_{yz}$ level is nonbonding since the $NH_3$ ligands have no available orbitals for $\pi$ bonding. The nearly equal energy of this level and the $d_{z^2}$ level indicates that participation of the $d_{z^2}$ orbital in $\sigma$ bonding must be slight. This is not unreasonable since this occupied orbital is antibonding and utilization would result in electronic destabilization. In contrast, the empty $d_{\sigma^*}$ orbital ($d_{x^2-y^2}$ in $D_{4h}$ or $D_{2h}$ or $d_{xy}$ in $C_{2v}$) is involved in $\sigma$ bonding to a considerable extent, causing the placement of this orbital at a high energy compared to the low-lying $\pi^*$ $CN^-$ orbitals. It is probable therefore that the burden of $\sigma$ bonding falls heavily on this orbital and the 6s, $6p_x$, and $6p_y$ orbitals in these and other square-planar complexes.

The shift of the $d_\pi$ levels lower than the virtually nonbonding $d_{z^2}$ level is reasonable for square complexes containing $\pi$-acceptor type ligands such as $CN^-$. Furthermore, the in-plane $d_{xy}$ level lies lower than the out-of-plane $d_{xz}d_{yz}$ levels in $Pt(CN)_4^{2-}$. The lower position for this orbital may be rationalized from a molecular orbital view point since it interacts with four $CN^-$ ligands compared to only two each in the case of $d_{xz}d_{yz}$. It is interesting that just the opposite behavior is found in the planar $PtX_4^{2-}$ ($X^- = Cl^-$ or $Br^-$) complexes where $L_\pi \rightarrow M$ ($\pi$ donation) is important.[5,25] The level ordering for these complexes is $d_{xy} > d_{xz}d_{yz} > d_{z^2}$ and places the $d_\pi$ levels higher in energy than the $d_{z^2}$ level. It should be pointed out though that the stabilization of the $d_\pi$ levels compared to $d_{z^2}$ in the cyano and cyanoamineplatinum complexes is not very large, amounting to no more than 5–7 kK. Consequently M

**Table V.** Metal → Ligand Charge Transfer and d → p Bands in Aqueous Solution[a]

| Complex | M → L |  |  |  |
|---|---|---|---|---|
|  | Band I | Band II | Band V | d → p |
| $Pt(CN)_4^{2-}$ [b] | 35.70 | 39.00 | 46.19[c] | >54 |
| *trans*-$Pt(NH_3)_2(CN)_2$ | 39.80 | 43.75 | 51.75 | 53.15 |
| *cis*-$Pt(NH_3)_2(CN)_2$ | 40.85 | 44.20 | 52.00 | *d* |
| $Pt(en)(CN)_2$ | 40.75 | 44.00 | 52.00 | *d* |
| Pt(*l*-pn)$(CN)_2$ | 41.00 | 44.00 | 51.75 | *d* |
| $Pt(dien)(CN)^+$ | 43.00 | 45.75 | *e* | 54.0 |
| $Pt(NH_3)_4^{2+}$ |  |  |  | 50.95[f] |

[a] Energies in kK. [b] Data from ref 5. [c] Band IV. [d] Insufficient data. [e] Obscured by the d → p transition. [f] Data from ref 19.

→ L π bonding cannot be a major factor in contributing to the bond strength of the Pt–CN bond.

The energies of the M → L charge-transfer bands in $Pt(CN)_4^{2-}$ and the cyanoamine complexes are related to the energy difference between the occupied metal d orbitals and the empty π* $CN^-$ acceptor orbital. The energies of the lowest energy and the two most intense bands in each complex are given in Table V. There is a distinct blue shift in each of these bands as the number of $CN^-$ ligands is reduced. This shift likely reflects an increase in metal d-orbital stability caused by an increase in metal charge as anionic $CN^-$ ligands are replaced by neutral N donors. Since the charge on the metal is related to the net flow of electron density from the ligands to the metal, the N donors act as weaker donor ligands than $CN^-$ toward the soft platinum(II) center. A similar conclusion can be drawn from formation constants for $NH_3$ and $CN^-$ complexes of other soft metal ions, where bonding is expected to be primarily dependent upon ligand donor character. Invariably the $NH_3$ complexes have lower formation constants than the $CN^-$ complexes. For example, $NH_3$ and $CN^-$ complexes of $CH_3Hg^+$ show values of $pK_{CH_3Hg^+}$ of 7.6 and 14.1, respectively.[26]

As shown also in Table V, the d → p transitions in *trans*-$Pt(NH_3)_2(CN)_2$ and $Pt(dien)(CN)^+$ are observed slightly higher in energy than the d → p transition in $Pt(NH_3)_4^{2+}$. The d → p transitions in $Pt(CN)_4^{2-}$ must be at energies higher than are accessible to measurement. The $6p_z$ orbital ($a_{2u}$ symmetry) in $Pt(NH_3)_4^{2+}$ is nonbonding. When $CN^-$ ligands are introduced into the complex, this orbital becomes antibonding and will be destabilized to the extent of the interaction with the π* orbitals. Therefore, d → p transitions are expected to be *higher* in energy than in the tetraammine complex, in agreement with experiment. The appearance of the d → p transitions only 3–4 kK higher in energy than for $Pt(NH_3)_4^{2+}$ suggests only a modest degree of interaction between the platinum $6p_z$ and the π* orbitals in the $Pt(dien)(CN)^+$ and *trans*-$Pt(NH_3)_2(CN)_2$ complexes. However, caution must be exercised in making quantitative statements about the extent of interaction because electron repulsion differences between M → L and d → p excited states are not known and may well be significantly different.

**Registry No.** $Pt(CN)_4^{2-}$, 15004-88-3; *trans*-$Pt(NH_3)_2(CN)_2$, 14095-76-2; *cis*-$Pt(NH_3)_2(CN)_2$, 14523-27-4; $Pt(en)(CN)_2$, 22924-94-3; Pt(*l*-pn)$(CN)_2$, 53965-97-2; $Pt(dien)(CN)^+$, 53965-98-3; *trans*-$Pt(NH_3)_2Cl_2$, 14913-33-8.

**Supplementary Material Available.** A listing of calculated spin–orbit eigenvalues and mixing coefficients, Table IV, will appear following these pages in the microfilm edition of this volume of the journal. Photocopies of the supplementary material from this paper only or microfiche (105 × 148 mm, 24× reduction, negatives) containing all of the supplementary material for the papers in this issue may be obtained from the Journals Department, American Chemical Society, 1155 16th Street, N.W., Washington, D.C. 20036. Remit check or money order for $3.00 for photocopy or $2.00 for microfiche, referring to code number AIC403915.

## References and Notes

(1) Abstracted in part from the Ph.D. dissertation of H. Isci, Northern Illinois University, 1974; presented in part at the XVIth International Conference on Coordination Chemistry, Dublin, Ireland, Aug 1974.

(2) C. K. Jorgensen, "Absorption Spectra and Chemical Bonding in Complexes," Addison-Wesley, Reading, Mass., 1962, p 198 ff.

(3) H. B. Gray and C. J. Ballhausen, *J. Amer. Chem. Soc.*, **85**, 260 (1963).

(4) C. Moncuit, *J. Chim. Phys. Physicochim. Biol.*, **64**, 494 (1967).

(5) W. R. Mason and H. B. Gray, *J. Amer. Chem. Soc.*, **90**, 5721 (1968).

(6) S. B. Piepho, P. N. Schatz, and A. J. McCaffery, *J. Amer. Chem. Soc.*, **91**, 5994 (1969); S. B. Piepho, Ph.D. Dissertation, University of Virginia, Charlottesville, Va., 1970.

(7) D. L. Webb and L. A. Rossiello, *Inorg. Chem.*, **10**, 2213 (1971).

(8) R. L. Musselman, Ph.D. Dissertation, New Mexico State University, Las Cruces, N.M., 1972.

(9) M. L. Moreau-Colin, *Struct. Bonding (Berlin)*, **10**, 167 (1972).

(10) K. Krogmann, *Angew. Chem., Int. Ed. Engl.*, **8**, 35 (1969).

(11) W. E. Cooley and D. H. Busch, *Inorg. Syn.*, **5**, 208 (1957).

(12) "Gmelins Handbuch der anorganischen Chemie," Vol. 68c, 8th ed, Verlag Chemie, Weinheim/Bergstr., Germany, 1930, p 201.

(13) O. N. Evstaf'eva, I. B. Baranovskii, and A. V. Babaeva, *Russ. J. Inorg. Chem.*, **10**, 14 (1965).

(14) H. L. Grube, "Handbook of Preparative Inorganic Chemistry," Vol. II, Georg Brauer, Ed., 2nd ed, Academic Press, New York, N.Y., 1965, p 1578. The thermal decomposition of $[Pt(NH_3)_4]Cl_2 \cdot H_2O$ was carried out at 200° rather than 250°; the product had a tendency to decompose at the higher temperature.

(15) I. B. Baranovskii and Yu. Ya. Kharitonov, *Dokl. Akad. Nauk SSSR*, **69**, 1335 (1966).

(16) Reference 12, p 123.

(17) G. W. Watt and W. A. Cude, *Inorg. Chem.*, **7**, 335 (1968).

(18) W. R. Mason, *J. Amer. Chem. Soc.*, **95**, 3573 (1973).

(19) H. Isci and W. R. Mason, *Inorg. Nucl. Chem. Lett.*, **8**, 885 (1972).

(20) Supplementary material.

(21) J. P. Mathieu and S. Cornevin, *J. Chim. Phys. Physicochim. Biol.*, **36**, 271 (1939).

(22) The coordinate system for this complex places the $C_2(x)$ axis along the Pt–CN bond. Therefore the $4a_1(x^2 - y^2)$ and $4b_2(xy)$ levels of Figure 1 are interchanged, and there will be only two π and two π* $CN^-$ levels, each of $b_1$ and $b_2$ symmetry.

(23) J. S. Griffith, "The Theory of Transition-Metal Ions," Cambridge University Press, Cambridge, England, 1964, p 438.

(24) C. K. Jorgensen, *Struct. Bonding (Berlin)*, **1**, 3 (1966), and references therein.

(25) R. F. Kroening, R. M. Rush, D. S. Martin, Jr., and J. C. Clardy, *Inorg. Chem.*, **13**, 1366 (1974).

(26) G. Schwarzenbach and M. Shellenberg, *Helv. Chim. Acta*, **48**, 28 (1965).